Available online at www.sciencedirect.com
SCIENCE DIRECT®
Reproductive Toxicology 19 (2005) 395–409
Reproductive Toxicology
www.elsevier.com/locate/reprotox

Modeling vitellogenesis in female fish exposed to environmental stressors: predicting the effects of endocrine disturbance due to exposure to a PCB mixture and cadmium

Cheryl A. Murphy[a,*], Kenneth A. Rose[a,b], Peter Thomas[c]

[a] *Department of Oceanography and Coastal Sciences, Energy, Coast and Environment Building, Louisiana State University, Baton Rouge, LA 70803, USA*
[b] *Coastal Fisheries Institute, Louisiana State University, Baton Rouge, LA 70803, USA*
[c] *Marine Science Institute, University of Texas at Austin, Port Aransas, TX 78373, USA*

Received 8 April 2004; received in revised form 20 September 2004; accepted 24 September 2004
Available online 14 November 2004

Abstract

A wide variety of chemical and physical environmental stressors have been shown to alter the reproductive processes in fish by interfering with endocrine function. Most endocrine indicators or biomarkers are static measures from dynamic hormonally-mediated processes, and often do not directly relate to reproductive endpoints of ecological significance. Adequate production of the yolk precursor protein, vitellogenin, is critical for the survival and normal development of the sensitive egg and yolk-sac larval fish life stages. We developed a model that simulates vitellogenesis in a mature female sciaenid fish. The model simulates the major biochemical reactions over a 6-month period from the secretion of gonadotropin (GtH) into the blood to the production of vitellogenin. We simulated the effects of two endocrine disrupting chemicals (EDCs) that have different actions on vitellogenin production: a PCB mixture and cadmium. Predicted changes in steroid concentrations and cumulative vitellogenin production compared favorably with changes reported in laboratory experiments. Simulations illustrate the potential utility of our model for interpreting reproductive endocrine biomarkers measured in fish collected from degraded environments.

Keywords: Vitellogenesis; Fish; Endocrine disrupting chemicals; Simulation model; Spotted seatrout; Steroid; Biomarker; Bioindicator

1. Introduction

There is now extensive evidence of reproductive and developmental abnormalities in fish and wildlife populations exposed to a wide variety of chemicals in the environment [1–3]. The aquatic environment is a sink for endocrine disrupting chemicals (EDCs) and other organic chemicals; therefore it is not surprising that there exist many examples of endocrine disruption in fish [3]. Fish immersed in the aquatic environment bioaccumulate lipophilic chemicals via ingestion from food items and via absorption of contaminants through their gills and scales. Among the many examples of endocrine disruptors that affect fish are man-made chemicals such as PCBs that affect the neuroendocrine system [4], and excessive concentrations of trace elements such as cadmium that can interfere with gonadotropin (GtH) regulation and steroidogenesis [5].

Fish play an integral role in the aquatic ecosystem food web, and any effects that change the population structure of fish may also alter community and food web dynamics. Because fish can biomagnify contaminants, fish are potentially useful sentinels of aquatic environmental degradation [6]. Fish carrying high loads of EDCs in their body tissue potentially suffer impaired health and can deliver high concentrations of EDCs to their consumers (i.e. apex predator

* Corresponding author. Tel.: +1 225 578 5970; fax: +1 225 578 6513.
E-mail address: cmurph4@lsu.edu (C.A. Murphy).

0890-6238/$ – see front matter © 2004 Elsevier Inc. All rights reserved.
doi:10.1016/j.reprotox.2004.09.006

species and humans). However, in many situations, the overall reproductive significance of the observed endocrine changes after exposure to EDCs remains unclear, and the potential ecological relevance is unknown.

Disturbances of reproductive function in field-caught female fish have been inferred from changes in endocrine and reproductive function biomarkers, such as altered sex steroid hormone, atypical gonadotropin and vitellogenin concentrations in circulation, and abnormal gonadal and oocyte growth. For example, fish exposed to bleached kraft pulp mill effluent showed changes in the induction of the hepatic mixed function oxygenase (MFO) enzyme system, reduced circulating levels of reproductive steroid hormones, reduced gonad growth, younger age to sexual maturation, and slower development of secondary sex characteristics. Examination of multiple biomarkers provides information on the exposure and reproductive health of the exposed fish [7,8].

Plasma concentrations of hormones taken at specified stages during the reproductive cycle can be a good indication of disruption of the reproductive process [9]. However, such biomarkers can be confounded by naturally occurring fluctuations in the reproductive cycle, and care must be taken when considering the timing of biomarker measurements [10]. Biomarkers are snapshots in time from a dynamic system. There is a need for models that can relate biomarker measurements to the entire reproductive cycle, and that can extrapolate biomarkers to ecologically relevant endpoints such as the production of eggs.

In this paper, we use a physiological model to simulate how two nonestrogenic EDCs that act via different mechanisms could affect vitellogenesis in fish. Vitellogenesis results in the production of the yolk precursor protein vitellogenin. Vitellogenesis is sensitive to disruption by EDCs and of ecological relevance because vitellogenin production is directly related to the reproductive output (fecundity and egg quality) of individual fish [11]. Our goal was to develop a modeling tool that quantitatively links relevant biomarkers of endocrine disruption in adult female fish to cumulative vitellogenin production over the reproductive season. We then used the model to simulate the effects of vitellogenin production of exposure to a PCB mixture and to cadmium. We base our computer model on two fish species from the family Sciaenidae: spotted seatrout (*Cynoscion nebulosus*) and Atlantic croaker (*Micropogonias undulatus*). Spotted seatrout and Atlantic croaker are well-established estuarine teleost model organisms used to study reproductive endocrinology and endocrine toxicity. Simulations illustrate how the model can be used to estimate the reproductive significance of endocrine biomarker measurements in field-caught fish. We are early in the process of model development, and our model should be considered as preliminary. Continued corroboration and testing, and targeted laboratory and field measurements, are planned to refine and improve the realism of the model.

2. Model description and simulations

2.1. Model overview

The model is a system of eight ordinary differential equations that simulate vitellogenesis in an individual mature female fish (Table 1; Fig. 1). The model is driven by the hourly introduction of gonadotropin and the resultant biochemical reactions are simulated for 6 months, resulting in a prediction of the cumulative production of vitellogenin. There is an equation for the rate of change of each of the eight state variables: free testosterone (T), unbound or free steroid binding protein (SBP), steroid binding protein bound to testosterone (SBP-T), steroid binding protein bound to estradiol (SBP-E2), free estradiol (E2), unbound or free estrogen receptor (ER), estrogen receptor bound to E2 or activated ER (ER-E2), and vitellogenin (Vtg).

There are also three additional differential equations that keep track of the output variables of total testosterone (free testosterone plus testosterone bound to steroid binding proteins), total estradiol (free estradiol plus estradiol bound to steroid binding proteins) and total estrogen receptor (free estrogen receptor plus estrogen receptor bound to estradiol). These output differential equations use the same processes as the state variables, but enable bookkeeping of the portion of the bound complexes that are the state variable of interest (e.g. how much testosterone is in the testosterone bound with the steroid binding protein state variable). Laboratory and field measurements are frequently reported as total concentrations, rather than the concentrations of the free and bound forms.

All of the state variable differential equations follow a standard format of expressing the rate of change of a

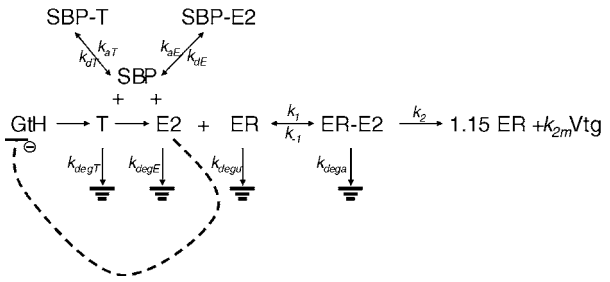

Fig. 1. Schematic representation of the major biochemical reactions represented in the model of vitellogenesis in an individual female fish. Gonadotropin (GtH) stimulates the production of testosterone (T), which provides a substrate for the production of estradiol (E2). T and E2 bind and unbind to steroid binding proteins (SBP) at rates of association (k_{aT}, k_{aE}) and rates of dissociation (k_{dT}, k_{dE}). Unbound steroids (free) are susceptible to degradation at specified rates (k_{degT}, k_{degE}). Free E2 binds to the estrogen receptor (ER) at a rate of k_1, forming an activated ER complex (E2-ER) and disassociates at rate of k_{-1}. High levels of E2 inhibit the production of GtH. The activated ER initiates a cascade of reactions that results in the production of more ER and (k_{2m} times) vitellogenin (Vtg) at a rate of k_2. Un-activated ER is susceptible to degradation at a rate of k_{degu}, whereas activated ER (E2-ER) degrades at a much faster rate (k_{dega}). A double arrow refers to a reversible reaction, a single arrow refers to an irreversible reaction, and the dotted line refers to inhibition.

state variable as equal to its synthesis rate minus degradation rate plus inactivation rate minus activation rate. All state variables and output variables are expressed as mass (pg or mg) per milliliter of blood (plasma), except for variables involving the estrogen receptor. The free estrogen receptor state variable (Eq. (7)) is reported in nM units. However, field measurements are reported in pico moles per gram of liver (pmol/g liver) [12]. We report the total estrogen receptor concentration output variable (Eq. (14)) in pico moles per gram of liver (pmol/g liver) to allow comparison to field measurements. Based on laboratory experiment protocol and dilutions, we multiplied

Table 1
System of ordinary differential equations that define the model of vitellogenesis in an individual mature female fish

Driving variable

$$\mathrm{GtH} = \frac{0.5\left(1 - 1.0\cos\frac{2\pi(t-6.0)}{24.0}\right)}{1.0 + \frac{[\mathrm{E2}]}{10}} \tag{1}$$

State variables

$$\frac{\mathrm{dT}}{\mathrm{d}t} = \mathrm{synT(GtH)} - k_{deg\mathrm{T}}[\mathrm{T}] + k_{\mathrm{dT}}[\mathrm{SBP-T}] - \mathrm{synE2(T)} - k_{a\mathrm{T}}[\mathrm{T}][\mathrm{SBP}] \tag{2}$$

$$\frac{\mathrm{dSBP}}{\mathrm{d}t} = k_{\mathrm{dT}}[\mathrm{SBP-T}] + k_{\mathrm{dE}}[\mathrm{SBP-E2}] - k_{a\mathrm{T}}[\mathrm{T}][\mathrm{SPB}] - k_{a\mathrm{E}}[\mathrm{E2}][\mathrm{SPB}] \tag{3}$$

$$\frac{\mathrm{dSBP-T}}{\mathrm{d}t} = k_{a\mathrm{T}}[\mathrm{T}][\mathrm{SBP}] - k_{\mathrm{dT}}[\mathrm{SBP-T}] \tag{4}$$

$$\frac{\mathrm{dSBP-E2}}{\mathrm{d}t} = k_{a\mathrm{E}}[\mathrm{E2}][\mathrm{SBP}] - k_{\mathrm{dE}}[\mathrm{SBP-E2}] \tag{5}$$

$$\frac{\mathrm{dE2}}{\mathrm{d}t} = \mathrm{synE2(T)} - k_{deg\mathrm{E}}[\mathrm{E2}] + k_{-1}[\mathrm{ER-E2}] + k_{\mathrm{dE}}[\mathrm{SBP-E2}] - k_1[\mathrm{E2}][\mathrm{ER}] - k_{\mathrm{aE}}[\mathrm{E2}][\mathrm{SBP}] \tag{6}$$

$$\frac{\mathrm{dER}}{\mathrm{d}t} = 1.15k_2[\mathrm{ER-E2}] - k_{degu}[\mathrm{ER}] + k_{-1}[\mathrm{ER-E2}] - k_1[\mathrm{E2}][\mathrm{ER}] \tag{7}$$

$$\frac{\mathrm{dER-E2}}{\mathrm{d}t} = k_1[\mathrm{E2}][\mathrm{ER}] - k_{dega}[\mathrm{ER-E2}] - k_{-1}[\mathrm{ER-E2}] - k_2[\mathrm{ER-E2}] \tag{8}$$

$$\frac{\mathrm{dVtg}}{\mathrm{d}t} = k_{2\mathrm{m}}k_2[\mathrm{ER-E2}] \tag{9}$$

where

$$\mathrm{synT(GtH)} = \frac{V_{1_\mathrm{T}}(\mathrm{GtH}^{h_\mathrm{T}})}{K_{m_\mathrm{T}}^{h_\mathrm{T}} + \mathrm{GtH}^{h_\mathrm{T}}} \tag{10}$$

$$\mathrm{synE2(T)} = \frac{V_{1_\mathrm{E}}(T^{h_\mathrm{E}})}{K_{m_\mathrm{E}}^{h_\mathrm{E}} + T^{h_\mathrm{E}}} \tag{11}$$

Output variables

$$\frac{\mathrm{dTotal\,T}}{\mathrm{d}t} = \mathrm{synT(GtH)} - k_{deg\mathrm{T}}[\mathrm{T}] - \mathrm{synE2(T)} \tag{12}$$

$$\frac{\mathrm{dTotal\,E2}}{\mathrm{d}t} = \mathrm{synE2(T)} - k_{deg\mathrm{E}}[\mathrm{E2}] + k_{-1}[\mathrm{ER-E2}] - k_1[\mathrm{E2}][\mathrm{ER}] \tag{13}$$

$$\frac{\mathrm{dTotal\,ER}}{\mathrm{d}t} = (0.15k_2[\mathrm{ER-E2}] - k_{degu}[\mathrm{ER}] - k_{dega}[\mathrm{ER-E2}])4.0\,\mathrm{L/g} \tag{14}$$

Eq. (1) is the equation for the single driving variable of gondadotropin concentration in the blood. Eqs. (2)–(9) correspond to each of the eight state variables in the model. Eqs. (10) and (11) are the Hill functions that appear in Eqs. (2) and (6), respectively. Eqs. (12)–(14) correspond to three output variables that use the same reactions as the state variables but allow for the reporting of total concentrations of testosterone, estradiol, and estrogen receptor.

nM units by 4.0 L/g to obtain the units of pmol/g liver [13].

The vitellogenic processes represented in the model are based on a very simplified view of the many biochemical reactions involved (Fig. 1). The model simulates the major reactions from the introduction of gonadotropin into the blood through the production of vitellogenin. Gonadotropin, which is produced in the pituitary, is released into the bloodstream where GtH travels to the ovary and stimulates thecal cells to produce testosterone. Free or unbound testosterone (T) is then converted to free estradiol (E2) in the neighboring ovarian granulosa cells [14]. Free testosterone and free estradiol rapidly associate with steroid binding proteins located in the plasma and form the SBP-T and SBP-E2 complexes. Once bound, testosterone and estradiol are protected from metabolic degradation; steroids in the free form (T and E2) are subjected to degradation. Free estradiol diffuses through tissues and acts at the pituitary and liver. In the pituitary, high levels of free estradiol inhibit the release of gonadotropin (dotted line in Fig. 1). In the liver, free estradiol associates with the estrogen receptor (ER) to form the estradiol-estrogen receptor complex (ER-E2). Small amounts of estradiol disassociate from the estrogen receptor and are re-introduced into the bloodstream. Activated estrogen receptor (ER-E2) is degraded. Activation of the estrogen receptor causes alterations in the rates of transcription of estrogen responsive genes leading to the synthesis of more estrogen receptor and vitellogenin (ER and k_{2m}Vtg).

We wanted a model prediction that could be interpreted as related to the total fecundity of an individual fish. Therefore, the model accumulates vitellogenin production over the simulation. In reality, vitellogenin concentration in the plasma varies over time, depending on both its production and its loss due to being taken up in rapidly growing oocytes. Vitellogenin is a yolk-precursor protein, and is an essential building block for oocytes and critical to the production of healthy eggs [15].

2.2. Model processes and parameter estimation

Below, we describe each of the major processes represented in the model, including the rationale for their formulations and the sources used to estimate model parameters. As much as possible, we use information from spotted seatrout and Atlantic croaker. Seatrout and croaker are both sciaenids, and have been well studied in a series of laboratory and field experiments [4,5,12,13,16–19]. Seatrout and croaker are both important estuarine species and croaker is widely distributed along most of the Atlantic coast extending up to Cape Cod [20,21]. In some instances, we used information from other species of fish. All equation numbers in the text refer to the equations listed in Table 1.

2.2.1. Gonadotropin

We used data on luteinizing hormone (LH) secretion as representative of gonadotropin in model simulations. Ovarian function in vertebrates, including oocyte and ovarian growth, is primarily regulated by gonadotropins secreted by the pituitary gland in response to neuroendocrine signals from the brain. As in most tetrapod vertebrates, the pituitary in teleosts produces two gonadotropins: follicle stimulating hormone (FSH) and LH [22]. Growth of the oocyte and ovarian follicle in tetrapods is primarily regulated by an increase in FSH secretion, whereas the physiological role of FSH (formerly GTH I) in regulating oocyte and ovarian follicle growth remains to be demonstrated in most teleost species. Salmonids are the only group of fishes for which a sensitive FSH radioimmunoassay has been developed. In salmonids, the secretion of FSH coincides with the period of gonadal growth, whereas LH secretion increases towards the end of the reproductive cycle roughly coinciding with oocyte maturation and spawning [23]. However, LH secretion in Atlantic croaker and several other teleosts shows diurnal changes and is under precise neuroendocrine control by transmitters, peptides, and steroids during ovarian growth [24,25]. Moreover, stressor-induced alterations in gonadal growth in Atlantic croaker have been associated with changes in LH secretion [4,26]. LH has similar steroidogenic potency to that of FSH at the gonadal growth stage of the reproductive cycle [27]. Although FSH has been identified in Atlantic croaker, no quantitative information is currently available on FSH secretion [28]. Taken together, these findings suggest a potential role for LH during ovarian and oocyte growth in Atlantic croaker. Therefore, data on LH secretion was used as representative of gonadotropin secretion, with the realization that we may need to revisit this issue as more data become available.

We represented LH concentrations in the plasma with a diurnal cycle based on observations on Atlantic croaker. During the period of gonadal recrudescence (which lasts about 8 weeks), LH plasma levels in croaker exhibit a diurnal pattern gradually reaching maximum values of about 1.0 ng/mL at dusk, and minimum values below detection by dawn (Thomas, unpublished data). We created a sinusoidal function to mimic the diurnal pattern of plasma gonadotropin concentration (numerator of Eq. (1); Fig. 2). The amount of

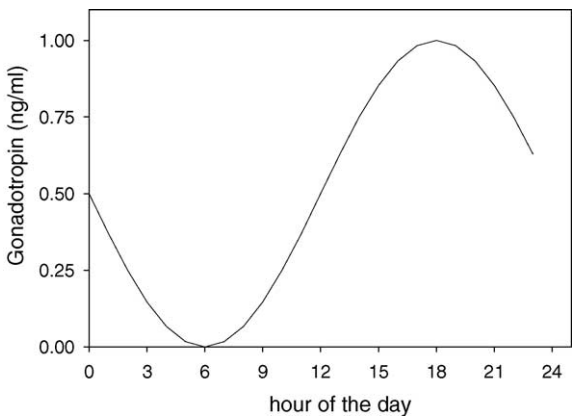

Fig. 2. Hourly concentrations of the gonadotropin driving variable showing the diurnal cycling assumed for the first 8 weeks of the baseline simulation.

gonadotropin produced by the sinusoidal function reflects the net plasma concentration of gonadotropin, and thereby accounts for degradation and removal. Gonadotropin was introduced for the first 8 weeks of the simulation, corresponding to the period of gonadal recrudescence, and then set to zero for the remainder of the simulation.

We also include a negative feedback by which steroids inhibit the introduction of the gonadotropin driving variable (denominator of Eq. (1)). Steroids such as testosterone and estradiol have been shown to have a negative feedback effect on FSH production in salmonids [29–31]. In Atlantic croaker, testosterone and estradiol stimulate LH production during early gonadal recrudescence, but inhibit the production of LH after gonad maturation [32]. Quantitative information is not available on the details of these positive and negative feedbacks. We do not model the estrogen receptor in the brain, but we incorporated the negative feedback mechanism into our model by reducing the plasma concentration of gonadotropin when free estradiol concentrations got very high. For example, a free estradiol concentration of 25 pg/mL plugged into the denominator of Eq. (1) would decrease the plasma gonadotropin concentration by 0.3%, and a higher concentration of 1000 pg/mL would decrease the plasma gonadotropin concentration by 9%.

2.2.2. Steroidogenesis

We opted for an aggregate approach to represent the many reactions involved in the stimulation of testosterone production by gonadotropin, and the subsequent use of testosterone for the production of estradiol. Many of the reactions involved have not been clearly defined. We therefore adopted the approach used by Schlosser and Selgrade [33], who aggregated many biochemical reactions into a few processes to model the synthesis of LH in humans and then used the model to predict the effects of EDCs on the human menstrual cycle. In our model, we lumped all of the reactions occurring between the release of gonadotropin and the production of testosterone into a general synthesis function (Eq. (10)), and we also grouped all of the reactions occurring between the release of testosterone and the production of estradiol into a second synthesis function (Eq. (11)). The basic form of both of these synthesis functions was a Hill equation, which exhibits a sigmoid relationship between substrate and product [34].

We estimated the parameter values of the Hill function that related gonadotropin concentration to testosterone production (Eq. (10)) from a study of steroidogenesis in goldfish [35]. In this study, the rate of testosterone production was obtained from pre-ovulatory follicles of goldfish incubated in increasing concentrations of carp gonadotropin. We derived the parameter values of the Hill function for the conversion of gonadotropin to testosterone by maintaining the shape of the relationship observed in the experiment with goldfish. The maximum testosterone production rate was chosen so that the assumed gonadotropin driving variable stimulated a maximum concentration of testosterone of about 1200 pg/mL within the first month of the baseline simulation. Smith and Thomas [12] reported a maximum total testosterone concentration of 1200 pg/mL in April in field-caught spotted seatrout. We tried a variety of values of V_1, K_m and h_t in Eq. (10) until we obtained set of values (Table 2) that produced a similarly shaped relationship between gonadotropin concentration and testosterone production rate as observed in the goldfish experiment but with concentrations pertinent to our baseline simulation (Fig. 3a).

To estimate the parameters for the second Hill function that related estradiol production to testosterone concentration, we maintained a sigmoidal shape to the function while constraining the function to occur within our simulated ranges of free testosterone concentration and free estradiol production. We used the range of free testosterone concentrations that occurred under baseline conditions in our model (0–100 pg/mL) because only 1–10% of the total testosterone is available as a ligand; much of testosterone and estradiol are bound to steroid binding proteins [36]. We assumed that testosterone is rapidly converted estradiol so that 23% is converted within 0.01 h; this assumption was based on a study by van der Kraak et al. [35] that reported estradiol production at high gonadotropin concentrations was approximately 23% of what would be the expected testosterone production from the same gonadotropin concentration. The value we assigned to V_{1E} (Table 2) was based on the assumption that at maximum concentrations of free testosterone (e.g. 100 pg/mL) estradiol production in one timestep of the model (0.0001 h) would be 0.23% of the maximum free testosterone concentration (i.e. 0.23 pg/mL/0.0001 h). We arbitrarily determined parameter values (K_m and h_E, Table 2) to maintain a sigmoid relationship between testosterone concentration and estradiol production (Fig. 3b).

2.2.3. Steroid binding proteins

Although steroid binding proteins have multiple functions, we only simulated their binding with free testosterone and free estradiol that resulted in steroids being protected from degradation. The main functions of steroid binding proteins appear to be to protect bound steroids from degradation, to regulate steroid uptake into the target tissue, and to participate directly in signal transduction [36–38]. However, because of limited information on the regulation and signal transduction functions, we only focused on the protection function of steroid binding proteins.

The kinetics of binding of estradiol and testosterone to the steroid binding proteins were represented with first order dissociation reactions and second order association reactions (Eqs. (3), (4) and (5)). We used equilibrium dissociation constants (K_d) reported by Laidley and Thomas [18] to estimate the model rate constants for the association and dissociation between testosterone and steroid binding proteins (k_{aT} and k_{dT}; Table 3), and between estradiol and steroid binding proteins (k_{aE}, and k_{dE}; Table 3). K_d is the ratio of the dissociation rate to the association rate, $K_d = k_{dissociation}/k_{association}$. The reported K_d of free testosterone with steroid binding pro-

Table 2
Definitions, relevant equation numbers, units, and baseline values of the parameters of the model of vitellogenesis in an individual female fish

Name	Definition	Equation	Units	Value
V_{IT}	Maximum rate of free testosterone production	10	pg/mL/h	80.0
V_{IE}	Maximum rate of free estradiol production	11	pg/mL/h	2300.0
K_{mT}	Half-saturation of free testosterone production	10	ng/mL	0.3
K_{mE}	Half-saturation of free estradiol production	11	pg/mL	52.0
h_T	Hill coefficient for free testosterone	10		1.8
h_E	Hill coefficient for free estradiol	11		3.5
k_{2m}	Multiplier for rate constant k_2	9		10.0
k_1	Association rate of free estradiol with estrogen receptor	6–8, 13	$1/10^8$ M/h	7.43
k_{-1}	Dissociation rate of free estradiol with estrogen receptor	6–8, 13	1/h	0.81
k_2	Rate of production of vitellogenin and estrogen receptor	7–9, 14	1/h	0.3465
k_{aT}	Association rate of free testosterone with steroid binding protein	2–4	$1/10^9$ M/h	5.6687
k_{dT}	Dissociation rate of free testosterone with steroid binding protein	2–4	1/h	27.72
k_{aE}	Association rate of free estradiol with steroid binding protein	4–6	$1/10^9$ M/h	5.6687
k_{dE}	Dissociation rate of free estradiol with steroid binding protein	4–6	1/h	17.74
k_{degT}	Degradation rate of free testosterone	2, 12	1/h	1.386
k_{degE}	Degradation rate of free estradiol	6, 13	1/h	1.386
k_{degu}	Degradation rate of free estrogen receptor	7, 14	1/h	0.00058
k_{dega}	Degradation rate of activated estrogen receptor	8, 14	1/h	0.012
Initial conditions for state variables that are different than 0				
T	Free testosterone	2	pg/mL	10.0
SBP	Free steroid binding protein	3	nM	400.0
E2	Free estradiol	6	pg/mL	10.0
ER	Free estrogen receptor	7	nM	0.125

teins was 4.89 nM, whereas estradiol had a greater affinity to steroid binding proteins with a reported K_d of 3.13 nM [18].

To separate the reported K_d values for estradiol with steroid binding proteins and for testosterone with steroid binding proteins into constituent association and dissociation rate constants, we first determined their dissociation rates. Laidley and Thomas [18] reported that radioactive testosterone had rapid association (half life or $t_{1/2} < 30$ s) and rapid dissociation ($t_{1/2}$ of about 90 s) with steroid binding proteins. We assumed k_{dT} was a first order rate constant, and then we solved for k_{dT} using the general relationship between the half-life ($t_{1/2}$) and the first-order rate constant (k): $t_{1/2} = 0.693/k$ [39]. Then, to determine the testosterone association rate constant with steroid binding proteins (k_{aT}), we divided k_{dT} by K_d. The association and dissociation rate constants of estradiol with steroid binding proteins was calculated assuming the association rate constant was the same as the association rate constant estimated for testosterone ($k_{aE} = k_{aT}$) and from the reported K_d for estradiol binding with steroid binding proteins reported by Laidley and Thomas [18].

We represented the dynamics of steroid binding proteins without synthesis or degradation reactions so that the total steroid binding protein concentration remained constant throughout the simulation. We fixed the total steroid binding protein concentration because, although the concentration of steroid binding protein increases with ovary maturation, their binding affinity to steroids decreases, suggesting a compensatory effect [19]. The initial concentration of total steroid binding protein was set to 400 nM, which corresponded to the mean value reported by Laidley and Thomas [19]. The percent of the total steroid binding protein found in the free

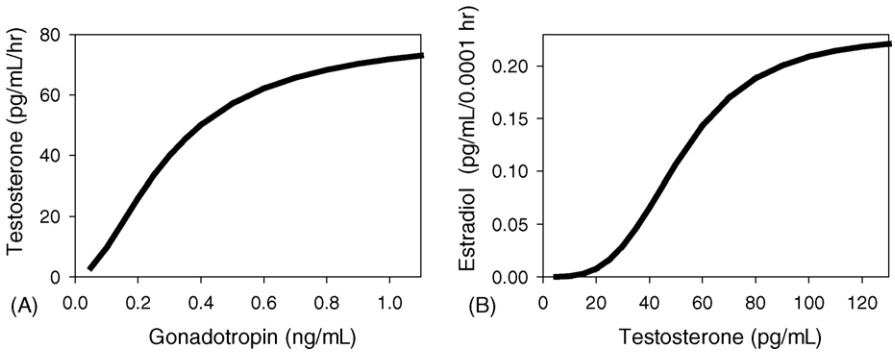

Fig. 3. Derived Hill functions for the production of free testosterone from gonadotropin and for the production of free estradiol from testosterone. (A) Simulated relationship between testosterone production and gonadotropin concentration; (B) simulated relationship between estradiol production and testosterone concentration.

Table 3
Predicted cumulative vitellogenin production of an individual female fish during 6-month simulations under baseline conditions, and under exposure to PCBs and cadmium

Simulation	Cumulative vitellogenin produced (mg/mL)	Percent of baseline (%)
Baseline	161.0	100
PCB	29.1	18
Cadmium	970.2	603

form versus bound to testosterone and to estradiol varied over time in the simulations.

Free testosterone (Eq. (2)) and free estradiol (Eq. (6)) are affected by synthesis (Eqs. (10) and (11)), interactions with steroid binding proteins (k_{aT}, k_{dT}, k_{aE}, k_{aE}), and undergo first order degradation (k_{degT}, k_{degE}). All of the biochemical reactions, except degradation, have been described. We assumed that the degradation rates for both steroids (k_{degT}, k_{degE}; Table 2) were 1.386/h. This degradation rate was calculated based upon the assumption that $t_{1/2}$ was 30 min, a value reported for the degradation rate of estradiol in salmonids [40].

2.2.4. Estrogen receptor and vitellogenin

We represented the binding of free estradiol to the estrogen receptor with first and second order kinetics. Free estradiol associates with the estrogen receptor using a second order rate constant (k_1) and dissociates from the estrogen receptor with a first order rate constant (k_{-1}) (Eqs. (6), (7) and (8)). The rate constants k_1 and k_{-1} (Table 2) were derived from values for K_d of 1.09 nM and k_{-1} of 0.0135/min reported for estradiol association and dissociation with estrogen receptor in spotted seatrout [13]. We calculated k_1 from the reported values of k_{-1} and K_d and then multiplied both k_{-1} and k_1 by 60 to create hourly rates (Table 2).

We calculated different degradation rates for the free and bound estrogen receptors. In mammals, degradation of free estrogen receptor depends on the presence of estradiol. In the absence of estradiol, degradation rates of estrogen receptor are relatively slow [41]. Smith and Thomas [13] reported a $t_{1/2}$ of 45 h or a rate of 0.0002/min for spotted seatrout. We used the degradation rate constant for the activated estrogen receptor (k_{dega}, Table 2) reported by Smith and Thomas [13], and calibrated the free estrogen receptor degradation rate (k_{degu}, Table 2) so that the maximum estrogen receptor concentration peaked at 5.25 pmol/g liver [see 12]

We assumed that one activated estrogen receptor resulted in the production of both vitellogenin (Eq. (9)) and more estrogen receptor (first term of Eq. (7)). We adopted a modeling approach used to model autocatalytic enzymatic reactions (e.g. Manjabacas et al. [42]). In this modeling approach, only one rate parameter (k_2) is required for the conversion of activated estrogen receptor to vitellogenin and more estrogen receptor. Although the exact length of time required to produce estrogen receptor protein is unknown, we estimated k_2 based on transcription rates for vitellogenin mRNA in rainbow trout where estrogen receptor mRNA transcription units reach 50% of maximum values by 2 h [43]. In order for the estrogen receptor to produce more of itself, the coefficient for the estrogen receptor must equal or exceed one. The magnitude of the coefficient affects the concentration of total estradiol; larger values lead to increased production of estrogen receptor that, in turn, results in a steeper decline in total estradiol concentration. We set the coefficient for the estrogen receptor to 1.15 (Fig. 1) in order to slow the decline in total estradiol concentration in the baseline simulation. Although production of estrogen receptor proceeds more rapidly than vitellogenin production, much more vitellogenin is produced than estrogen receptor [43]; but the exact quantities are unknown. Therefore, we assigned a value of 10 to the multiplier of vitellogenin (i.e. $k_{2m} = 10$) to initially get appropriate predictions of final cumulative concentrations of vitellogenin. The value of k_{2m} was not adjusted further during calibration.

2.3. Model simulations

Three model simulations were performed that illustrate the utility of the model for understanding the effects of endocrine disruptors on vitellogenesis in fish. The first simulation was for baseline, or unstressed, conditions. We used the results of long-term field measurements to calibrate the model (adjusted values of V_{1T}, k_{degu}, and the coefficient of estrogen production as described below) until model predictions roughly mimicked the dynamics observed in field-caught fish. The two remaining simulations involved simulating the effects of PCB mixture (Aroclor 1254) and cadmium. These stressors differ on how they affect vitellogenin production. For each of these stressors, we compared predicted dynamics of selected state and output variables between baseline and stressed simulations, and also compared model-predicted changes in cumulative vitellogenin production to changes in the gonadal somatic index (GSI) measured in laboratory experiments. GSI is based on percent of gonadal weight divided by body weight, and is a commonly used measure of reproductive functioning in fish [44].

All model simulations were for 6 months duration covering the period roughly from 1 April through 1 October, which is the spawning season of spotted seatrout in the northern Gulf of Mexico [45]. The system of differential equations was solved using a 4th order Runge–Kutta method with a numerical time step of 0.0001 h; values of each of the eight state variables and three output variables were outputted every hour for the 6 months. A small numerical time step was used because some of the reactions were very rapid.

2.3.1. Calibration and baseline conditions

We calibrated the model for baseline conditions based on the values of total testosterone, total estradiol, and total estrogen receptor measured monthly over 2 years in field-caught spotted sea trout [12]. We compared model predictions to the values measured between April and October because this was when total testosterone, total estradiol, and total estrogen

receptor were near or at their maximum concentrations. We also show the dynamics of free testosterone and free estradiol to illustrate model dynamics. The baseline model simulation used the standard diurnal introduction of gonadotropin (Fig. 2) for the first 8 weeks of the simulation.

Calibration focused on three model parameters: the synthesis rate of testosterone (V_{1T} in Eq. (10)), the degradation rate of free estrogen receptor (k_{degu} in Eq. (7)) and the coefficient for the production of estrogen receptor (1.15 in Fig. 1 and in Eq. (7)). Values of all model parameters were originally derived from the literature. We adjusted V_{1T}, k_{degu}, and the coefficient of estrogen production in repeated model simulations until predicted maximum values of total testosterone, total estradiol, and total estrogen receptor were similar in magnitude and occurred in approximately the same month as observed in the field measurements. All other parameters were maintained at the values originally derived from the literature.

2.3.2. Effects of PCBs

We simulated the effects of the PCB mixture (Aroclor 1254) exposure using the results of laboratory experiments performed on Atlantic croaker [4,16,17]. Aroclor 1254 affects fish hypothalamic–pituitary–gonadal–liver axis at multiple sites [46]. However, in this analysis we only focused on the PCB effect on gonadotropin releasing hormone functioning and luteinizing hormone secretion; in Atlantic croaker, Aroclor 1254 inhibits tryptophan hydroxylase activity [4]. In a laboratory experiment, adult croaker were acclimated for 1 month and then were exposed to Aroclor 1254 (2 ug/g body weight per day) for 15 days during early gonadal recrudescence [4]. Plasma levels of LH measured after the 15 days of exposure were 38% of the values of the control fish.

Two earlier studies that examined the effects of PCBs on Atlantic croaker documented reduced GSI and testosterone, and somewhat opposite effects on estradiol concentrations. Female Atlantic croaker exposed to Aroclor 1254 (5 ug/g body weight per day) for 17 days during early gonadal recrudescence had GSI values and total estradiol levels that were roughly 50% lower than in control fish [17]. In another experiment, female Atlantic croaker were also exposed to Aroclor 1254 (3.5 ug/g body weight per day), but for a longer 30-day exposure [16]. GSI levels were 34% and total testosterone concentrations that were 50% of control values, but plasma estradiol concentrations were 25% higher than in control fish [16]. The contrasting PCB effects on total estradiol levels can be explained, in part, by the different durations (17 and 30 days) of the two experiments. Under PCB exposure, estradiol could initially be reduced due to reduced gonadotropin release, and then increase later in the season due to PCBs affecting a different mechanism of the HPLG axis other than gonadotropin release.

To simulate the effects of PCBs, we multiplied the plasma gonadotropin driving variable concentrations by 0.38. We compared predicted model dynamics under PCB exposure to baseline results. We compared predicted changes in testosterone, estradiol and cumulative vitellogenin production to the roughly 50% reductions in testosterone, estradiol and GSI observed in the lab experiments.

2.3.3. Effects of cadmium

Cadmium appears to disrupt vitellogenesis in fish at multiple steps. Cadmium acts on both the pituitary and the gonad to alter gonadotropin secretion and steroidogenic activity [5,17]. Female croaker acclimated for 30 days and then exposed to cadmium in vivo (1 mg/L) for 40 days showed 295% higher GtH concentrations and 211% higher total estradiol concentrations as compared to control fish [17]. Ovarian fragments of spotted seatrout were incubated in various concentrations of cadmium in vitro [5]. Incubation in cadmium in vitro, at a range of cadmium exposures (range from 0.01 to 5.0 ppm) that should encompass the exposure level imposed in the in vivo Thomas [17] study on croaker, resulted in a doubling of testosterone production after 9 h, and a doubling of estradiol production after 18 h.

To simulate the endocrine disrupting effects of cadmium, we increased the plasma concentration of gonadotropin and the rate of testosterone synthesis (conversion of gonadotropin to testosterone). The gonadotropin concentration was increased by multiplying the hourly baseline values (Fig. 2) by 2.95, as observed in the in vivo experiment [17]. The testosterone synthesis rate was increased by multiplying Eq. (10) by 2.0 (Table 1), as observed in the in vitro ovarian fragment incubation experiment [5]. We assumed that a doubling of the testosterone synthesis rate would roughly translate into a doubling of estradiol production that was also observed in the in vivo [17] and in vitro ovarian fragment [5] experiments. We compared model predictions under baseline and cadmium exposure, and compared predicted cadmium effects on cumulative vitellogenin production to changes in GSI reported by Thomas [17].

3. Results

3.1. Calibration and baseline conditions

The calibrated baseline simulation predicted magnitudes and timing of peak concentrations of total estrogen receptor, total testosterone, and total estradiol that roughly mimicked those measured in spotted seatrout by Smith and Thomas [12]. Model-predicted cumulative vitellogenin production under baseline conditions was 161.0 mg/mL (Fig. 4a; Table 3). Measured estrogen receptor concentration peaked at about 2 pmol/g liver in September during the first year of measurements and had a higher and longer duration peak (5.25 pmol/g liver for May through September) during the second year of measurements. In the baseline simulation, predicted total estrogen receptor concentration, while increasing throughout the period of gonadotropin introduction in the simulation, approached a maximum concentration of 5.2 pmol/g liver by the middle of the simulation that was

similar magnitude to the field measured concentrations (Fig. 4b). Measured total testosterone reached a maximum concentration of about 1200 pg/mL sometime between April and June, and then declined slowly to about 300 pg/mL by October to November. Predicted total testosterone peaked in the baseline simulation at 1290 pg/mL within the first month of simulation (April), remained elevated during the period of gonadotopin release and then declined rapidly to zero, contrasting field measurements that measured minimum concentrations of 300 pg/mL (Fig. 4c). Finally, over the 2 years of observations, total estradiol attained a maximum concentration of about 1750 pg/mL sometime during May and July. Predicted total estradiol concentration in the baseline simulation peaked at 1800 pg/mL during April (Fig. 4d).

Although detailed measurements concerning concentrations of the free forms of testosterone and estradiol are not available, model predictions of very low concentrations of these were consistent with general observations. Petra et al. [36] reported that in mammals only a small percentage (about 1%) of free steroids are available as a ligand at any given time; much of available steroid is bound to SBP. Maximum predicted free testosterone concentration in the baseline simulation was 15.8 pg/mL (Fig. 4e), which was about 1.2% of the total testosterone concentration. Similarly, predicted concentrations of free estradiol reached a maximum of 14.2 pg/mL (Fig. 4f), which was about 0.8% of the maximum total estradiol concentration.

The temporal dynamics of the free forms of testosterone and estradiol were consistent with the model structure and assumed parameter values. Rapid fluctuations in free estradiol (Fig. 4f) and testosterone (Fig. 4e) were due to hourly variation in gonadotropin concentration over the diurnal cycle, values of parameter (k_{aT}, k_{dT}, k_{aE} and k_{dE}) that resulted in rapid association and dissociation of the free forms with steroid

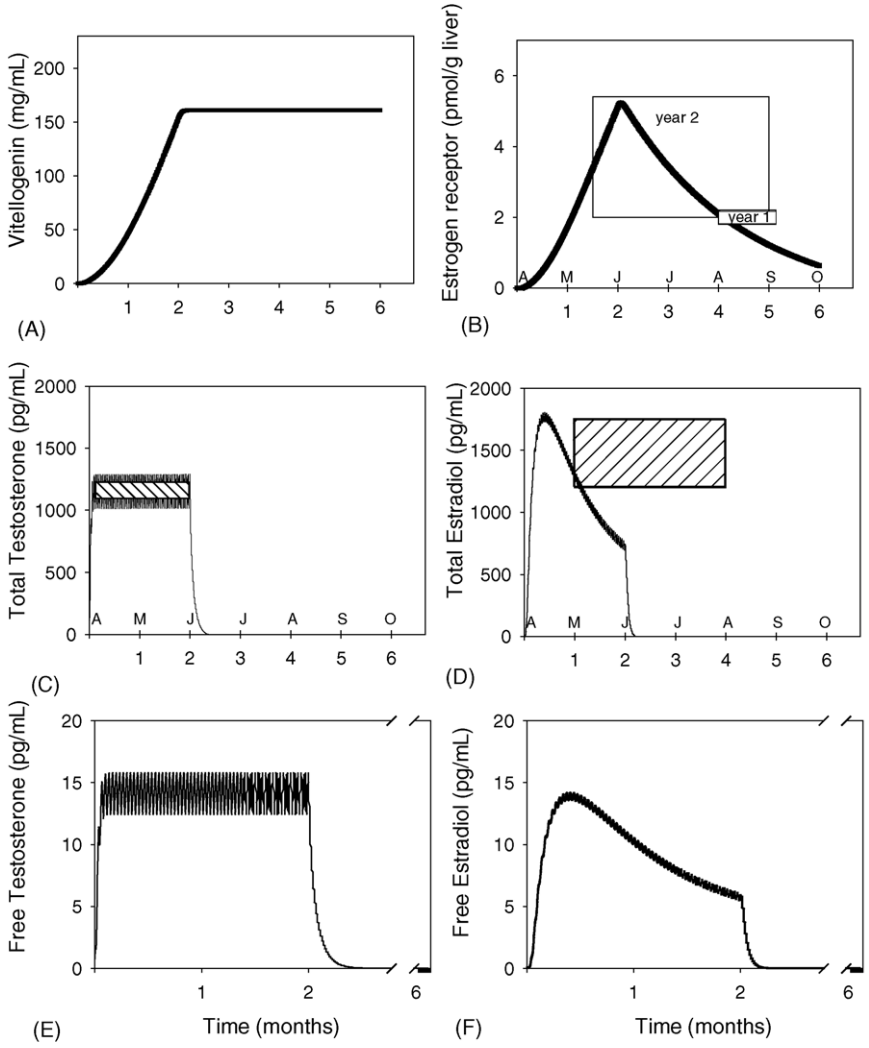

Fig. 4. Baseline simulation predictions of: (A) cumulative vitellogenin production; (B) estrogen receptor concentration; (C) total estradiol; (D) total testosterone concentration; (E) free testosterone concentration; and (F) free estradiol concentration. Boxes represent ranges of field-measured maximum concentrations. The small box in (B) represents the range of peak concentrations of total estrogen receptor observed in first year of field measurements, and the large box represents the range of peak concentrations of total estrogen receptor observed in the second year of field measurements. The hatched box in (C) represents the peak reported concentrations of total testosterone, and the hatched box in (D) represents the range in reported peak total estradiol concentrations.

binding proteins, the rapid degradation rates of free testosterone and estradiol (k_{degu} and k_{dega}), and the fast reaction rates of testosterone and estradiol as substrates in subsequent reactions. The initial rapid rise of free estradiol concentrations during the first month of the simulation (Fig. 4f) was due to the rapid synthesis of estradiol from the rapid increase in concentration of free testosterone.

3.2. Effects of PCBs

Predicted reduction in cumulative vitellogenin production due to PCB exposure was higher compared to the observed reductions in GSI documented in the laboratory experiments (Fig. 5a). Predicted cumulative vitellogenin production was 18% of baseline (Table 3), compared to the 34–50% reductions in GSI reported by Thomas [16,17].

Predicted estrogen receptor concentration was reduced under PCB exposure (Fig. 5b). Predicted total estrogen receptor showed similar dynamics under PCB exposure and baseline conditions of gradually rising concentrations during gonadotropin introduction, with maximum concentrations under PCB exposure reaching 13% of baseline by the middle of the simulation.

Predicted changes in total testosterone and estradiol concentrations were either consistent or equivocal when compared to the experimental results. PCBs were predicted to cause a 26% decrease in maximum total testosterone concentrations (Fig. 5c), which is roughly comparable to the 50% reduction in peak total testosterone concentrations reported by Thomas [17]. Predicted response to PCBs reflected a 62% decrease in total estradiol concentrations (Fig. 5d). This reduction in total estradiol is consistent with the interpretation of an initial reduction in estradiol in the shorter duration experiment [17] but is inconsistent with the increase in estradiol observed in the longer duration experiment [16]. The discrepancy between the two experimental results may be related to differences in their durations or perhaps to other differences in experimental design or protocol.

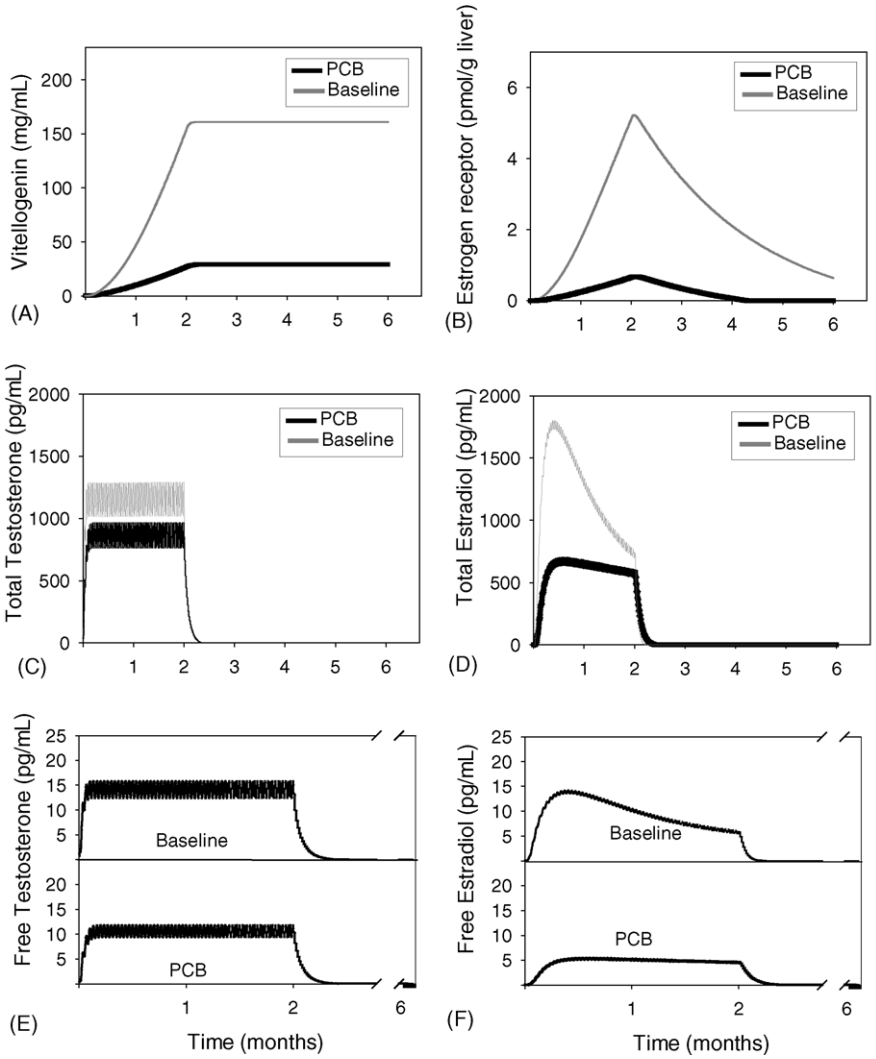

Fig. 5. Predicted concentrations under PCB exposure and baseline conditions of: (A) vitellogenin; (B) total estrogen receptor; (C) total testosterone; (D) total estradiol; (E) free testosterone; and (F) free estradiol.

Predicted responses in other state variables to PCB exposure were reduced free testosterone (Fig. 5e) and reduced free estradiol (Fig. 5f) concentrations. Free estradiol and free testosterone under PCB exposure both showed reductions in their peak concentrations compared to baseline conditions, with free testosterone and free estradiol reaching peak concentration that were 75 and 38% of the baseline peak concentration, respectively.

3.3. Effects of cadmium

Cadmium exposure caused large increases in vitellogenin production in both the model simulation and in the laboratory experiment. Predicted cumulative vitellogenin production was 603% higher than under baseline conditions (Table 2, Fig. 6a). Thomas [17] reported that cadmium exposed fish had GSIs that were 931% higher than control values (GSI of 1.16% in control versus 10.8% in cadmium exposed).

The imposition of higher rates of gonadotropin introduction and testosterone synthesis assumed under cadmium exposure resulted in increased total estrogen receptor concentrations, total testosterone, and total estradiol concentrations. Total estrogen receptor concentrations behaved similarly under cadmium exposure and baseline conditions, but attained maximum concentrations 6.2 times higher under cadmium exposure than under baseline conditions (Fig. 6b). Predicted total testosterone concentrations under cadmium exposure increased similar to baseline conditions, but attained a slightly higher maximum concentration at 1.4 times baseline (Fig. 6c). Predicted total estradiol concentrations under cadmium exposure rose more rapidly and maintained maximum concentrations at 3.2 times that of baseline conditions (Fig. 6d).

Free testosterone and free estradiol concentrations also reached higher peak concentrations under cadmium exposure than under baseline conditions. Free testosterone concentrations under cadmium exposure peaked at a concentration 1.4

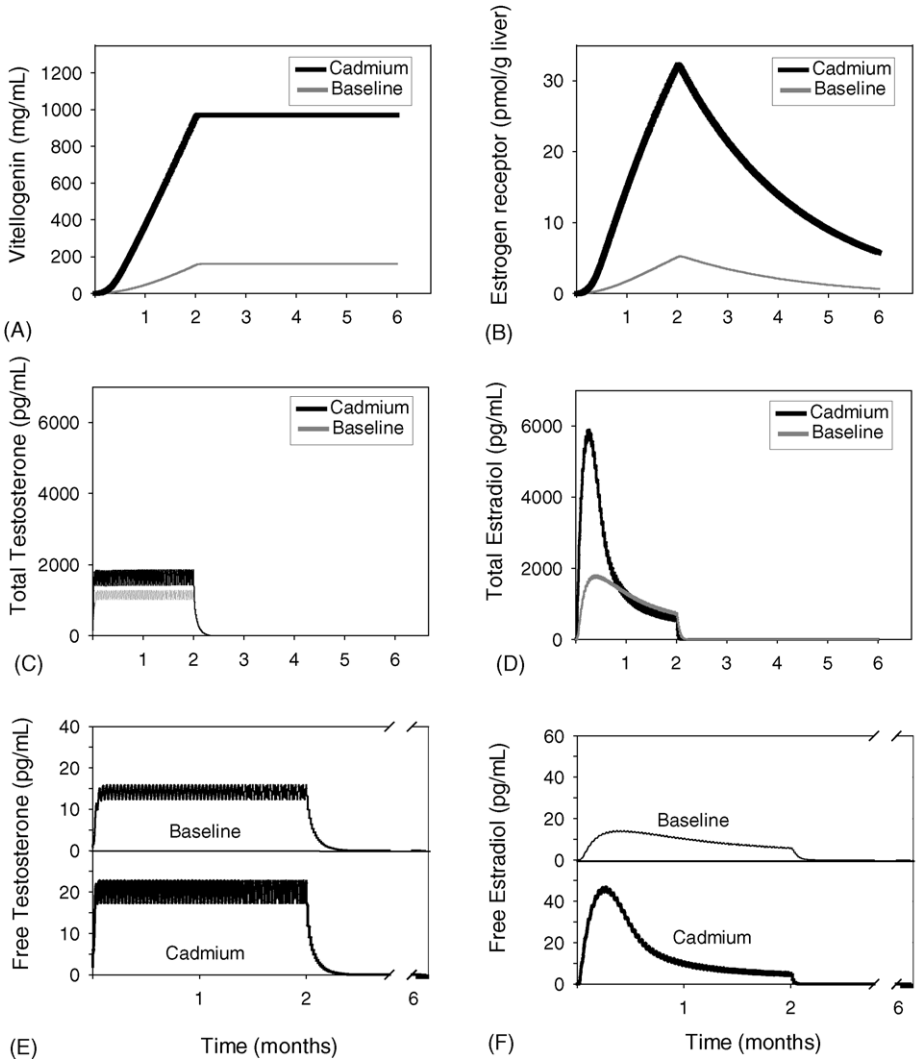

Fig. 6. Predicted concentrations under cadmium exposure and baseline conditions of: (A) vitellogenin; (B) total estrogen receptor; (C) total testosterone; (D) total estradiol; (E) free testosterone; and (F) free estradiol.

times that of baseline conditions (Fig. 6e). Free estradiol levels were more sensitive to cadmium exposure and reached a maximum at 3.3 times that observed under baseline conditions (Fig. 6f).

4. Discussion

4.1. Model performance and utility

We developed a model of vitellogenesis for an individual fish, and used the model to predict the effects of two EDCs. The model performed reasonably well. Baseline predictions of maximum concentrations of total steroids and estrogen receptor roughly matched field measurements, and predicted changes in vitellogenin production and estradiol levels under PCB and cadmium exposure generally matched changes observed in laboratory measurements of GSI and estradiol concentrations. The prediction of reduced vitellogenin production under PCB exposure may have been higher than observed in laboratory experiments because the simulation assumed PCB exposure during entire simulation, whereas in laboratory experiments fish were exposed to PCBs for only a portion of the reproductive period Also, based on our experience with measurements in field-caught seatrout, the baseline simulation wrongly predicted a decline to zero concentration of total testosterone and estradiol, rather than to some basal low concentrations, and predicted a peak in total estradiol concentration that occurred a few weeks too early (Fig. 4c and d).

Our simulations of contaminant effects demonstrated the need to recognize the importance of timing in biomarker measurement. Steroid concentrations in plasma are commonly used as biomarkers of exposure [47]. According to our model simulations, measurements of steroid levels from contaminant exposed fish that were taken during the first 2 months of gonadal recrudescence would show the greatest difference from control fish and that estradiol is a more sensitive biomarker than testosterone. Previous research indicates that depressed steroid levels translate into reproductive impairment (e.g. McMaster et al. [10]). Therefore, proper interpretation of estradiol concentrations from field-caught fish is predicated upon knowing the stage in the reproductive cycle of the individual fish.

The simulation of cadmium effects demonstrated how the model could be used to simulate EDCs that affect multiple sites on the hypothalamus–pituitary–gonad–liver (HPGL) axis. Cadmium affects the HPGL axis at the pituitary by stimulating the release of LH, and cadmium also acts on the ovary to enhance steroidogenesis [5]. We simultaneously imposed both of these effects in our cadmium exposure simulation. We doubled the concentration of gonadotropin in the plasma and doubled the rate of synthesis of testosterone.

A logical extension of how we simulated multiple effects of cadmium would be the simulation of exposure to multiple EDCs. Our model can be used to explore the possibility of synergistic and antagonistic effects. Fish in nature are exposed to mixtures of chemicals at various concentrations. For example, kelp bass (*Paralabrax clathratus*) that were collected from Southern California were environmentally exposed to mixtures of DDT and PCBs [48]. Exposed fish exhibited suppressed gonadotropin secretion from pituitary consistent with PCB effects. But the same fish also showed enhanced ovarian production of testosterone and reduced estrogen receptor affinity to estradiol, effects that could be attributed to other contaminants and may counteract the effects of PCBs. Spies and Thomas [48] reported that exposure to DDT and PCBs resulted in no noticeable reduction in vitellogenesis or GSI. *p*,*p*′-DDE, a metabolite of DDT which binds to the kelp bass androgen receptor [49], exerts anti-androgenic effects in vertebrates [50]. *p*,*p*′-DDE comprised over 95% of the total DDT detected in the contaminated kelp bass tissues [48]. Therefore, it would be necessary to include androgen-receptor mediated endocrine disruption in our model to simulate the multiple effects observed in the kelp bass. The model would also require modification for simulating the effects of the large number of chemicals that exert estrogenic actions via binding to the estrogen receptor to alter vitellogenesis and other reproductive processes.

4.2. Assumptions and deficiencies

Despite our use in model development of many laboratory experiments performed over decades, there are several aspects of the model that deserve careful scrutiny and further refinement. Perhaps one of the most useful outcomes of developing a model such as ours is the identification of data gaps and assumptions that need further confirmation.

We borrowed techniques from the field of enzyme kinetics [34] to model the dynamics of the estrogen receptor and steroid binding proteins. Enzyme kinetics was the starting point when researchers set out to generate models for epidermal growth factor (EGF) receptor binding and internalization [51]. The initial steady state and kinetic models were successful at capturing many of the dynamic features of the EGF binding processes. Once a model framework was built, models were expanded upon as technology improved and more data became available [51]. We view our model of vitellogenesis as analogous to the initial kinetic models of the EGF binding processes. We used simple first and second order rate constants for receptor association and dissociation processes, and we borrowed from an autocatalytic enzyme kinetics model example [42] to model the estrogen receptor producing more of itself.

One major uncertainty in our model is the identity of the principal gonadotropin regulating vitellogenesis in the sciaenid fish model. The effects of changes in LH secretion were modeled in this preliminary version of the model. This assumption may be correct for sciaenid fishes as well as some other marine perciform fishes such as European sea bass and red seabream [52]. However, our use of LH would

clearly be inappropriate for salmonids, and probably some other species in which FSH appears to regulate vitellogenesis [23]. Currently, the physiology of FSH secretion during ovarian growth has only been investigated in salmonid fishes due to the lack of immmunoassays for FSH measurement in members of other teleost families. Thus, in the absence of information on the pattern of FSH secretion during vitellogenesis in additional fish species, the role of FSH in the regulation of ovarian growth in teleosts remains unclear.

Experiments that determine the rates of synthesis of testosterone and estradiol in vitellogenic follicles in vivo would be useful for model refinement. In our model, rates of synthesis of testosterone and estradiol were calibrated to generate desired maximum concentrations of these steroids in the baseline simulation. However, rates of steroidogenesis may change with time and a gradual decline in rates of steroid synthesis or induction of other mechanisms, such as steroidogenic enzymes, may generate the slow decline in total testosterone and estradiol concentrations observed in field-caught fish. Further exploration into the mechanisms regulating steroidogenesis is required for more realistic simulations.

Another area in model development that required questionable assumptions was the steroid feedback mechanisms that affected gonadotropin production and release. We know that high doses of estradiol, administered through implants, inhibit the production of gonadotropin, but dose–response studies designed to quantify feedback mechanisms are not available. Steroid feedback mechanisms in Atlantic croaker have been studied, but not sufficiently to allow inclusion into our model. Information obtained through gonadectomy and steroid implants showed that during early gonad recrudescence, testosterone and estradiol stimulate LH production. However, when gonads reach maturation, the steroids inhibit the production of LH [32]. Information on the positive feedback exhibited early in gonadal recrudescence was insufficient, and we therefore only incorporated the negative feedback mechanism into our model. We simply assumed that high concentrations of estradiol would act to reduce gonadotropin levels.

Measurement of the degradation rate for estrogen receptors when estradiol is present would also be helpful. Hepatic estrogen receptor, in the presence of estradiol, undergoes degradation at a different rate than when estradiol is absent [41]. Therefore, we modified the estrogen receptor degradation rates so that the estrogen receptor concentration approached a maximum concentration near the middle of the baseline simulation. Experiments that determine the degradation rates for estrogen receptor in the absence of estradiol in seatrout would allow more precise parameter values to be used in model simulations.

The apparent disconnect between model predictions of estradiol concentrations and the results of laboratory experiment that used a longer PCB exposure period could be attributed to PCB affecting mechanisms other than gonadotropin release. We greatly simplified the effects of PCBs by assuming PCBs only affect gonadotropin release, whereas in reality PCBs affect many components of the HPGL axis [46].

The vitellogenesis model was calibrated to simulate baseline conditions from field-caught spotted seatrout, but data from toxicology studies on Atlantic croaker were also used. Although both species are estuarine species from the family Sciaenidae, they exhibit different life history strategies. Spotted seatrout will spawn multiple times in a season, whereas Atlantic croaker will only spawn once [53]. Because we are only modeling vitellogenesis and not the production and spawning of eggs, we felt it was reasonable to synthesize information from both spotted seatrout and Atlantic croaker for model development. Also, when we simulated the toxicology experiments we focused on percent changes in hormones rather than on changes in actual concentrations. Regardless, we recognize that hormonal profiles may differ between spotted seatrout and croaker, and these differences act as a source of error in the model.

4.3. Future directions

In addition to model refinement as data gaps are filled, we would also like to extend the model to include simulations of other mechanisms of endocrine disruption, especially those involving binding to nuclear estrogen or androgen receptors and alterations of steroid actions. Many major environmental contaminants bind to the estrogen receptor and are estrogenic (xenoestrogens), and there is extensive evidence of inappropriate induction vitellogenesis in fish by xenoestrogens in both field and laboratory studies. Endocrine disrupting chemicals can also interfere with later phase of the ovarian cycle such as oocyte maturation and spawning. For example, Kepone and *o*,*p*′-DDD bind to the maturation inducing steroid (4-pregnen-17,20β,21-triol-3-one) receptor sites and inhibit final oocyte maturation [54]. Also, as information becomes available, some of the aggregated biochemical reactions, like the Hill functions and the rate of production of vitellogenin and estrogen receptor, can be broken down into their component reactions. The Hill function has been used previously as a surrogate to model detailed biochemical reactions by Schlosser and Selgrade [33], and it is a reasonable approach because the sigmoid relationship observed between ligand concentration and product has been observed in many biochemical systems. Although the relationship between product and substrate is generally linear, it is convoluted by binding dynamics, degradation, and ligand depletion, thereby indirectly giving rise to the observed sigmoid shape [51]. Breaking the Hill function into components would likely increase the realism of the model, and allow us to easily simulate additional endocrine disrupting effects, such as the aromatase impairment associated with hypoxia exposure [55] and effects on steroid binding proteins [56].

We presented deterministic predictions in this paper. In future versions of our model, we plan to use Monte Carlo methods to include stochasticity (natural variability) and uncertainty in model predictions. Monte Carlo methods involve

repeated model simulations with input values randomly generated from probability distributions. Model predictions are then presented as probability distributions of outcomes, and correlation analysis can be used to identify the inputs that most contribute to prediction variability (e.g. Jaworska et al. [57]).

Ultimately, we would like to couple our model with a bioenergetics model of fish growth. Bioenergetics models are based on dynamic energy budgets and can be used to describe the rates at which individuals allocate energy for maintenance, reproduction, growth, and development [58,59]. In many bioenergetics models, the mechanisms determining energy allocation between somatic growth and reproduction are not well understood and usually determined by simple rules [60]. Coupling our vitellogenesis model to a bioenergetics model would allow simulation of the effects of endocrine disruption on energy allocation, and the resulting ecological consequences on reproduction and growth. Incorporation of endocrine disrupting effects into a coupled reproduction-bioenergetics model can eventually be used to relate biomarkers to population and community responses. The model presented in this paper is a first step towards a computational biology framework for a better understanding of endocrine disruption in fish, and for relating reproductive endocrine biomarkers of exposure to reproductive endpoints of ecological relevance.

5. Disclaimer

Although the research described in this article has been funded wholly or in part by the United States Environmental Protection Agency through cooperative agreement R 829458 to CEER-GOM, it has not been subjected to the Agency's required peer and policy review and therefore does not necessarily reflect the views of the Agency and no official endorsement should be inferred.

Acknowledgements

This research has been supported by a grant from the US Environmental Protection Agency's Science to Achieve Results (STAR) Program through funding from US EPA Agreement (R 827399) and from the STAR and Estuarine and Great Lakes (EaGLe) program through funding to (CEER-GOM), US EPA Agreement (R 829458). The authors also thank two anonymous reviewers for helpful comments on the manuscript.

References

[1] Colborn T, Saalvom FS, Soto AM. Developmental effects of endocrine-disrupting chemicals in wildlife and humans. Environ Health Perspect 1993;101:378–84.

[2] WHO. Global assessment of the state-of-the-science of endocrine disruptors. In: Damstra, T, Barlow, S, Bergman, A, Kavlock, R, van der Kraak, G, editors. International programme on chemical safety; 2002.

[3] Kime DE. Endocrine disruption in fish. Norwell, MA: Kluwer Academic Publishers; 2001.

[4] Khan IA, Thomas P. Disruption of neuroendocrine control of luteinizing hormone secretion by Aroclor 1254 involves inhibition of hypothalmic tryptophan hydroxylase activity. Biol Reprod 2001;64:955–64.

[5] Thomas P, Khan IA. Mechanisms of chemical interference with reproductive endocrine function in sciaenid fishes. In: Rolland RM, Gilbertson M, Peterson RE, editors. Chemically induced alterations in functional development and reproduction of fishes. Racine, WI: SETAC Technical Publications Series; 1995. p. 29–51.

[6] Davis WP. Evidence for developmental and skeletal responses as potential signals of endocrine-disrupting compounds in fishes. In: Rolland RM, Gilbertson M, Peterson RE, editors. Chemically induced alterations in functional development and reproduction of fishes.. Racine, WI: SETAC Technical Publications Series; 1995. p. 61–72.

[7] Munkittrick KR, Portt CB, van der Kraak G, Smith IR, Rokosh DA. Impact of bleached kraft mill effluent on population characteristics, liver MFO activity, and serum steroid levels of a Lake Superior white sucker (*Catostomus commersoni*) population. Can J Fish Aquat Sci 1991;48:1371–80.

[8] McMaster ME, van der Kraak GJ, Munkittrick KR. An epidemiological evaluation of the biochemical basis for steroid hormonal depressions in fish exposed to industrial wastes. J Great Lakes Res 1996;22:153–71.

[9] Donaldson EM. Reproductive indices as measures of the effects of environmental stressors in fish. Am Fish Soc Symp 1990;8:109–22.

[10] McMaster ME, Jardine JJ, Ankley GT, et al. An interlaboratory study on the use of steroid hormones in examining endocrine disruption. Environ Toxicol Chem 2001;20:2081–7.

[11] Tyler CR, Sumpter JP. Oocyte growth and development in teleosts. Rev Fish Biol Fisheries 1996;6:287–318.

[12] Smith JS, Thomas P. Changes in hepatic estrogen-receptor concentration during the annual reproductive and ovarian cycles of a marine teleost, the spotted seatrout *Cynoscion nebulosus*. Gen Comp Endocrinol 1991;81:234–45.

[13] Smith JS, Thomas P. Binding characteristics of the hepatic estrogen receptor of the spotted seatrout, *Cynoscion nebulosus*. Gen Comp Endocrinol 1990;77:29–42.

[14] Nagahama Y. Endocrine regulation of gametogenesis in fish. Int J Dev Biol 1994;38:217–29.

[15] Specker JL, Sullivan CV. Vitellogenesis in fishes: status and perspectives. In: Davey KG, Peter RE, Tobe SS, editors. Perspectives in comparative endocrinology. Ottawa: National Research Council; 1994. p. 304–15.

[16] Thomas P. Reproductive endocrine function in female Atlantic croaker exposed to pollutants. Mar Environ Res 1988;24:179–83.

[17] Thomas P. Effects of Aroclor 1254 and cadmium on reproductive endocrine function and ovarian growth in Atlantic croaker. Mar Environ Res 1989;28:499–503.

[18] Laidley CW, Thomas P. Partial characterization of a sex-steroid binding protein in the spotted seatrout (*Cynoscion nebulosus*). Biol Reprod 1994;51:982–92.

[19] Laidley CW, Thomas P. Changes in plasma sex steroid-binding protein levels associated with ovarian recrudescence in the spotted seatrout (*Cynoscion nebulosus*). Biol Reprod 1997;56:931–7.

[20] Diamond SL, Crowder LB, Cowell LG. Catch and bycatch: the qualitative effects of fisheries on population vital rates of Atlantic croaker. Trans Am Fish Soc 1999;128:1085–105.

[21] Diamond SL, Cowell LG, Crowder LB. Population effects of shrimp trawl bycatch on Atlantic croaker. Can J Fish Aquat Sci 2000;57:2010–21.

[22] Suzuki K, Kawauchi H, Nagahama Y. Isolation and characterization of two distinct gonadotropins from chum salmon pituitary glands. Gen Comp Endocrinol 1988;71:292–301.
[23] Swanson P. Salmon gonadotropins: reconciling old and new ideas. In: Scott AP, Sumpter J, Kime D, Rolfe MS, editors. Proceedings 4th International Symposium on Reproductive Physiology of Fish, 1991. p. 2–7.
[24] Khan IA, Thomas P. GABA exerts stimulatory and inhibitory influences on gonadotropin II secretion in the Atlantic croaker (*Micropogonias undulatus*). Neuroendocrinology 1999;69:261–8.
[25] Copeland PA, Thomas P. Control of gonadotropin release in the Atlantic croaker: evidence for lack of dopaminergic inhibition. Gen Comp Endocrinol 1989;74:474–83.
[26] Khan IA, Thomas P. Lead and Aroclor 1254 disrupt reproductive neuroendocrine function in Atlantic croaker. Mar Environ Res 2000;50:119–23.
[27] Patino R, Yoshizaki G, Thomas P, Kagawa H. Gonadotropic control of ovarian follicle maturation: the two stage concept and its mechanisms. Comp Biochem Physiol B 2001;129:427–39.
[28] Copeland PA, Thomas P. Isolation of gonadotropin subunits and evidence for distinct gonadotropins in Atlantic croaker (*Micropogonias undulatus*). Gen Comp Endocrinol 1993;91:115–25.
[29] Breton B, Sambroni E, Govoroun M, Weil C. Effects of steroids on GTH I and GTH II secretion and pituitary concentration in the immature rainbow trout *Oncorhynchus mykiss*. CR Acad Sci Paris. Sciences de la vie. 1997;320:783–9.
[30] Dickey JT, Swanson P. Effects of sex steroids on gonadotropin (FSH and LH) regulation in coho salmon (*Oncorhynchus kisutch*). J Mol Endocrinol 1998;21:291–306.
[31] Saligaut C, Linard B, Mananos EL, Kah O, Breton B, Govoroun M. Release of pituitary gonadotrophins GtH I and GtH II in the rainbow trout (*Oncorhynchus mykiss*): modulation by estradiol and catecholamines. Gen Comp Endocrinol 1998;109:302–9.
[32] Khan IA, Hawkins MB, Thomas P. Gonadal stage-dependent effects of gonadal steroids on gonadotropin II secretion in the Atlantic croaker (*Micropogonias undulatus*). Biol Reprod 1999;61:834–41.
[33] Schlosser PM, Selgrade JF. A model of gonadotropin regulation during the menstrual cycle in women: qualitative features. Environ Health Perspect 2000;108:873–81.
[34] Segel IH. Enzyme kinetics. In: Behavior and analysis of rapid equilibrium and steady-state enzyme systems. New York: Wiley; 1975.
[35] van der Kraak G, Suzuki K, Peter RE, Itoh H, Kawauchi H. Properties of common carp gonadotropin I and gonadotropin II. Gen Comp Endocrinol 1992;85:217–29.
[36] Petra PH, Stanczyk FZ, Namkung PC, Fritz MA, Novy MJ. Direct effect of sex steroid-binding protein (SBP) of plasma on the metabolic clearance rate of testosterone in the rhesus macaque. J Steroid Biochem 1985;22:739–46.
[37] Pardridge WM. Transport of protein-bound hormones into tissues in vivo. Endocr Rev 1981;2:103–23.
[38] Rosner W. The functions of corticosteroid-binding globulin and sex hormone-binding globulin: recent advances. Endocr Rev 1990;11:80–91.
[39] McQuarrie DA, Rock PA. General chemistry. 2nd ed. New York: W. H. Freeman and Company; 1987.
[40] Zohar Y. L'évolution de la pusatilité et des cycles nycthémérau de la sécrétion gonadotrope chez la truite arc-en-ciel femelle, en relation avec le cycle sexuel annuel et par rapport a l'activité stéroidogène de l'ovaire. Ph.D. thesis. Paris: Université Pierre et Marie Curie; 1982.
[41] Reid G, Denger S, Kos M, Gannon F. Human estrogen receptor-α: regulation by synthesis, modification and degradation. Cell Mol Life Sci 2002;59:821–31.
[42] Manjabacas MC, Valero E, Moreno-Conesa M, Garcia-Moreno M, Molina-Alarcon M, Varon R. Linear mixed irreversible inhibition of the autocatalytic activation of zymogens. Kinetic analysis checked by simulated progress curves. Int J Biochem Cell Biol 2002;34:358–69.
[43] Flouriot G, Pakdel F, Valotaire Y. Transcriptional and post-transcriptional regulation of rainbow trout estrogen receptor and vitellogenin gene expression. Mol Cell Endocrinol 1996;124:173–83.
[44] Barton BA, Morgan JD, Vijayan MM. Physiological and condition-related indicators of environmental stress in fish. In: Adams SM, editor. Biological indicators of aquatic ecosystem stress. Bethesda, MD: American Fisheries Society; 2002. p. 111–48.
[45] Brown-Peterson NJ. The reproductive biology of the spotted seatrout. In: Bortone SA, editor. Biology of the Spotted Seatrout. Boca Raton, FL: Marine Biology Series; 2003. p. 99–133.
[46] Thomas P. Molecular and biochemical responses of fish to stressors and their potential use in environmental monitoring. Am Fish Soc Symp 1990;8:9–28.
[47] Monosson E. Reproductive and developmental effects of PCBs in fish: a synthesis of laboratory and field studies. Rev Toxicol 2000;3:25–75.
[48] Spies RB, Thomas P. Reproductive and endocrine status of female kelp bass from a contaminated site in the Southern California Bight and estrogen receptor binding of DDTs. In: Rolland RM, Gilbertson M, Peterson RE, editors. Chemically induced alterations in functional development and reproduction of fishes. Racine, WI: SETAC Technical Publications Series; 1995. p. 113–33.
[49] Sperry T, Thomas P. Identification of two nuclear androgen receptors in kelp bass (*Paralabrax clathratus*) and their binding affinities for xenobiotics: comparison with Atlantic croaker (*Micropogonias undulatus*) androgen receptors. Biol Reprod 1999;61:1152–61.
[50] Kelce WR, Stone CR, Laws SC, Gray LE, Kemppainen JA, Wilson EM. Persistent DDT metabolite *p,p′*-DDE is a potent androgen receptor antagonist. Nature 1995;375:581–5.
[51] Wiley HS, Shvartsman SY, Lauffenburger DA. Computational modeling of the EGF-receptor system: a paradigm for systems biology. Trends Cell Biol 2003;13:43–50.
[52] Okuzawa K. Puberty in teleosts. Fish Physiol Biochem 2002;26: 31–41.
[53] Thomas P, Arnold CR, Holt GJ. Sciaenid fishes. In: Bromage N, Roberts RH, editors. Broodstock management and egg and larval quality. Blackwell Scientific Publishers; 1995. p. 118–37.
[54] Das S, Thomas P. Pesticides interfere with the nongenomic action of a progestogen on meiotic maturation by binding to its plasma membrane receptor on fish oocytes. Endocrinology 1999;140:1953–6.
[55] Wu RSS, Zhou BS, Randall DJ, Woo NYS, Lam PKS. Aquatic hypoxia is an endocrine disruptor and impairs fish reproduction. Environ Sci Technol 2003;37:1137–41.
[56] Tollefsen K-E. Interaction of estrogen mimics, singly and in combination, with plasma sex steroid-binding proteins in rainbow trout (*Oncorhynchus mykiss*). Aquat Toxicol 2002;56:215–25.
[57] Jaworska JS, Rose KA, Brenkert AL. Individual-based modeling of PCBs effects on young-of-the-year largemouth bass in southeastern USA reservoir. Ecol Model 1997;99:113–35.
[58] Ney JJ. Bioenergetics modeling today: growing pains on the cutting edge. Trans Am Fish Soc 1993;122:736–48.
[59] Nisbet RM, Muller EB, Lika K, Kooijman SALM. From molecules to ecosystems through dynamic energy budget models. J Anim Ecol 2000;69:913–26.
[60] Hewett SJ, Johnson BL. Fish bioenergetics model 2. University of Wisconsin Sea Grant Technical Report; 1992 [WIS-SG-92-250].